Supplement of Hydrol. Earth Syst. Sci., 26, 6457–6476, 2022
https://doi.org/10.5194/hess-26-6457-2022-supplement


Hydrology and Earth System Sciences
Open Access

*Supplement of*

# Global evaluation of the "dry gets drier, and wet gets wetter" paradigm from a terrestrial water storage change perspective

**Jinghua Xiong et al.**

*Correspondence to:* Shenglian Guo (slguo@whu.edu.cn)

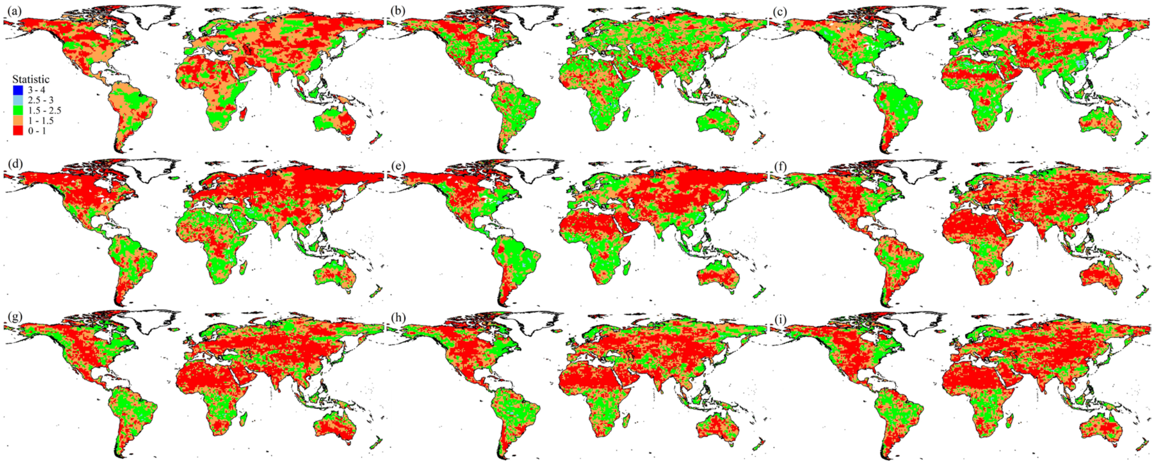


**Figure S1** Global assessment of the autocorrelation during the (a-f) historical (1985-2014) and future (2071-2100) period under (g) SSP126, (h) SSP245, and (i) SSP585 scenarios. Note: The historical results are based on the (a) GRACE reconstruction, (b) WGHM, (c) VIC, (d) CLSM, (e) Noah, and (f) ensemble mean of eight GCMs, respectively using the Durbin-Watson test. The future results are based on the ensemble of eight GCMs. Generally, the residuals are considered not auto-correlated when the Durbin-Watson test statistic has a value between 1.5 and 2.5. If the statistic is below 1 or above 3, then there is definitely autocorrelation among the residuals.

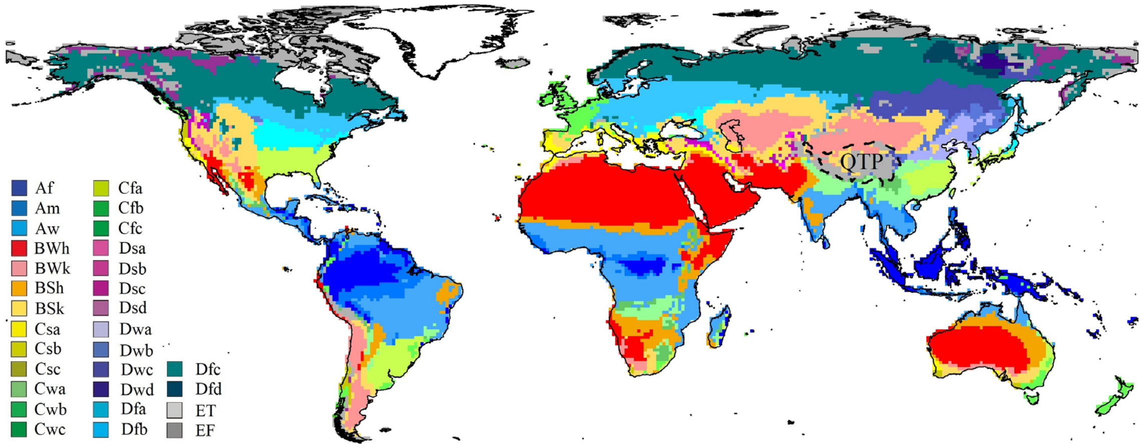


**Figure S2.** Global distribution of the improved Köppen-Geiger classifications during the period 1980-2016. Note: Please refer to Beck et al. (2018) for the details of the classification criteria. The dashed boundary represents the Qinghai-Tibetan Plateau.

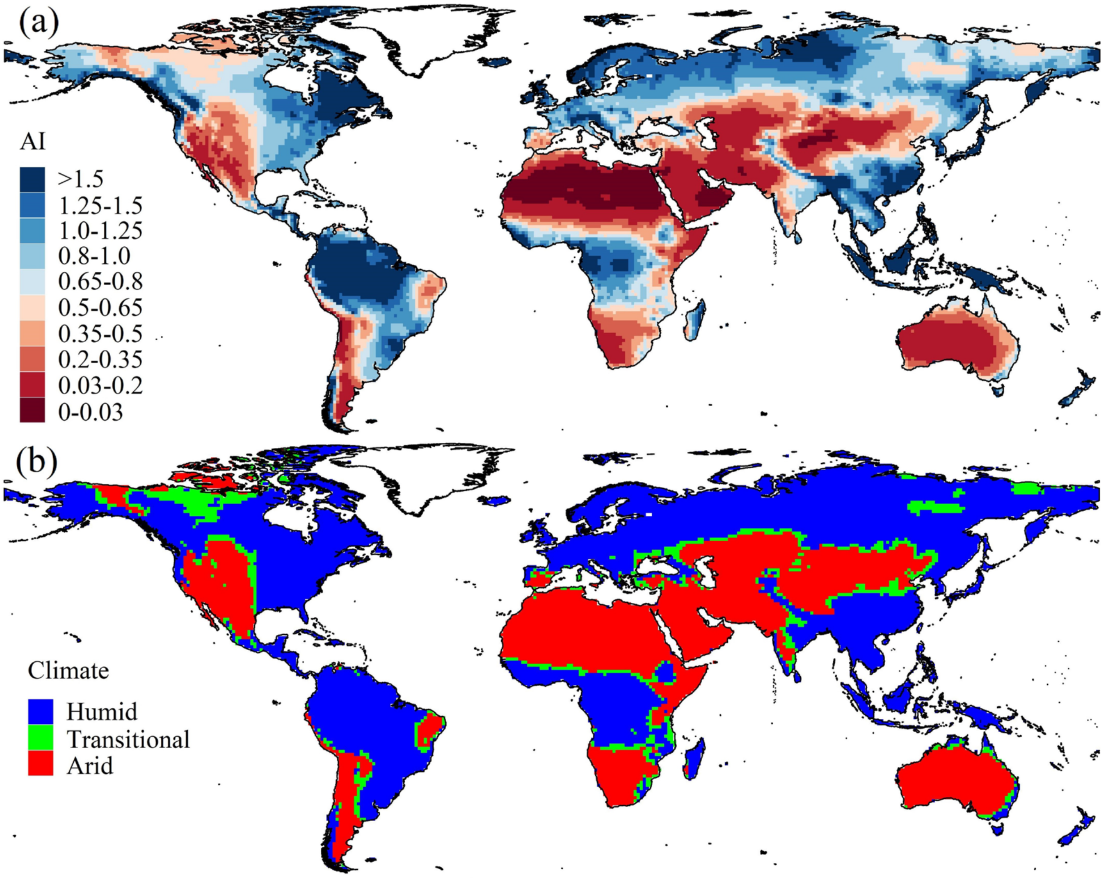


**Figure S3.** Global distribution of the (a) multi-year average aridity index (AI) and (b) climate type during the period 1985-2014. Note: The regions where AI>0.65 and <0.50 are defined as humid and arid regions, respectively.

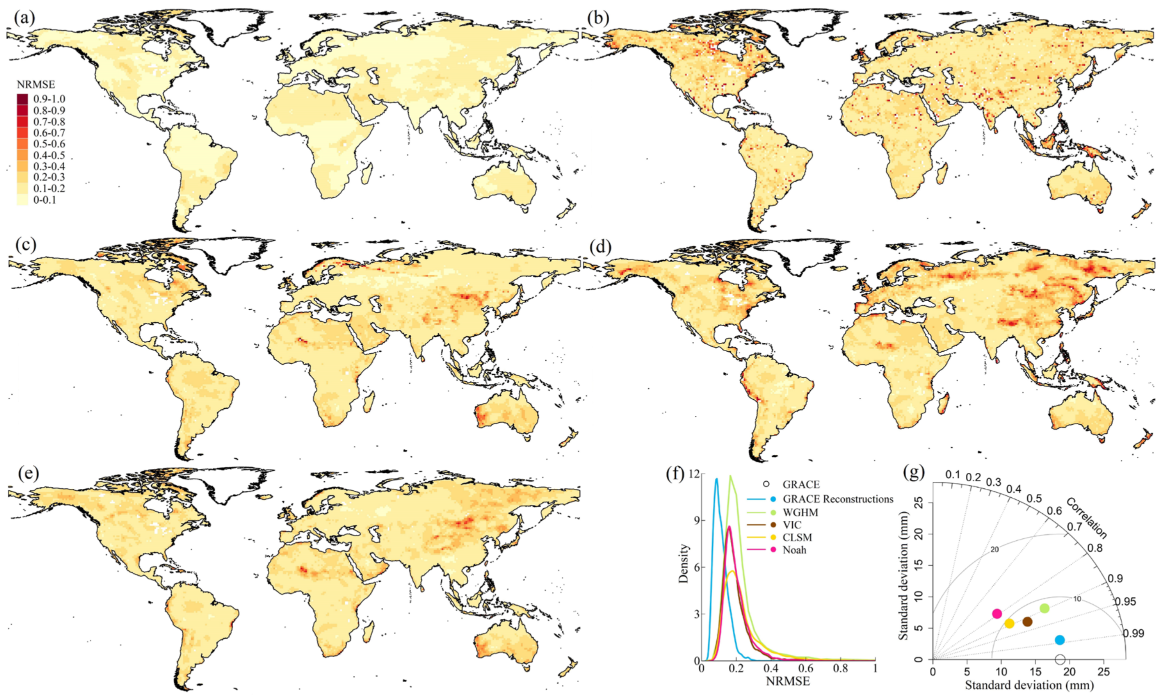


**Figure S4.** (a-e) Global distribution and (f) probability density function of the normalized root mean square error (NRMSE) and (g) Taylor diagram between TWSA derived from the GRACE observations and (a) GRACE reconstruction, (b) WGHM, (c) VIC, (d) CLSM, and (e) Noah models during the period April 2002-December 2014.

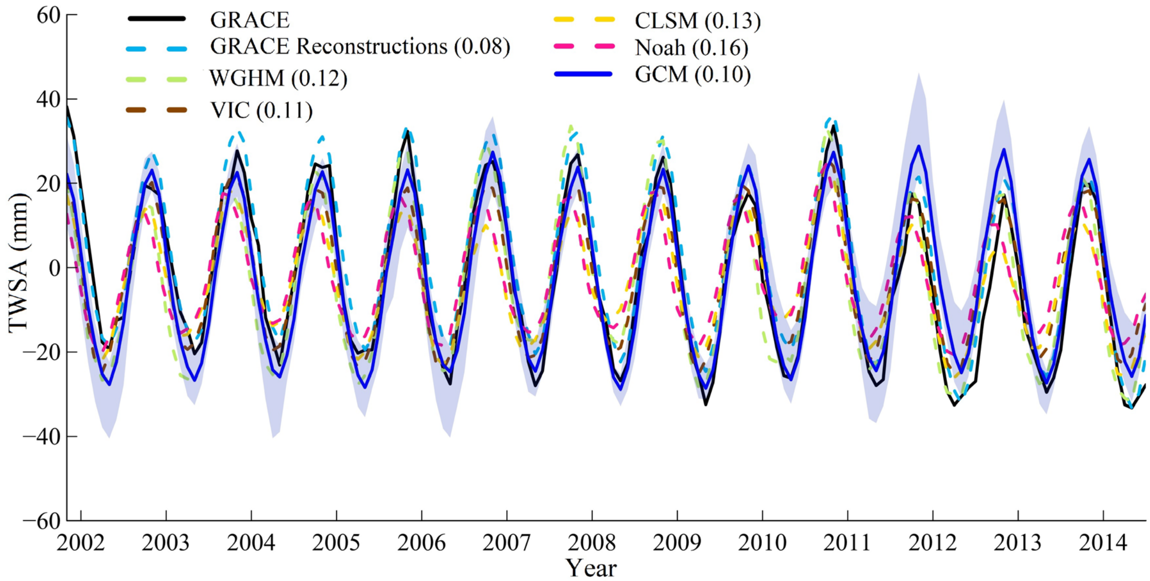


**Figure S5.** Time series of monthly TWSA derived from the GRACE products and different TWSA datasets over the global land excluding Antarctica and Greenland during the period April 2002-December 2014. Note: NRMSE between GRACE and different datasets are also shown. The deep blue line denotes the ensemble mean of eight GCMs. The shaded areas represent the range of TWSA values among the individual GCM datasets.

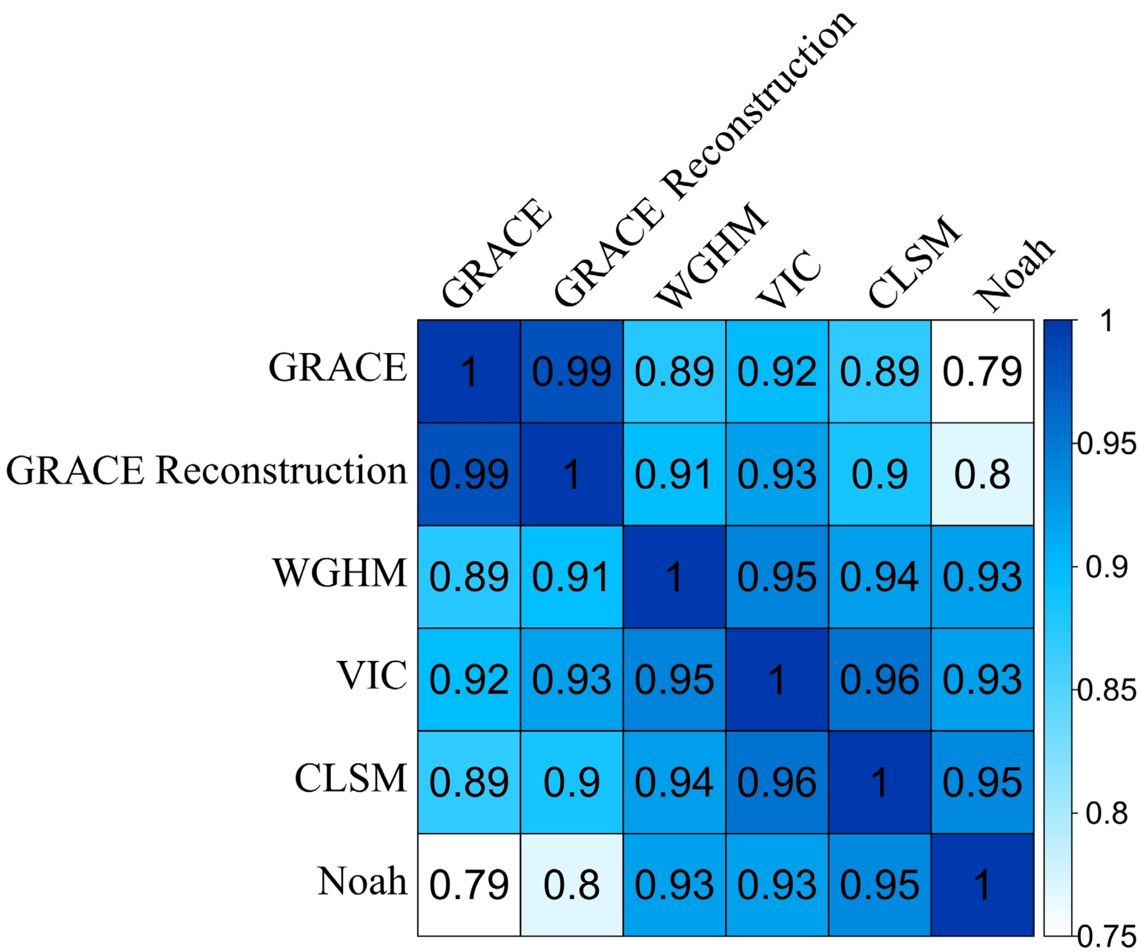


**Figure S6.** Correlation matrix between different datasets and GRACE over global land excluding Antarctica and Greenland during April 2002-December 2014. Note: The numbers mean the Pearson correlation coefficients within two variables.

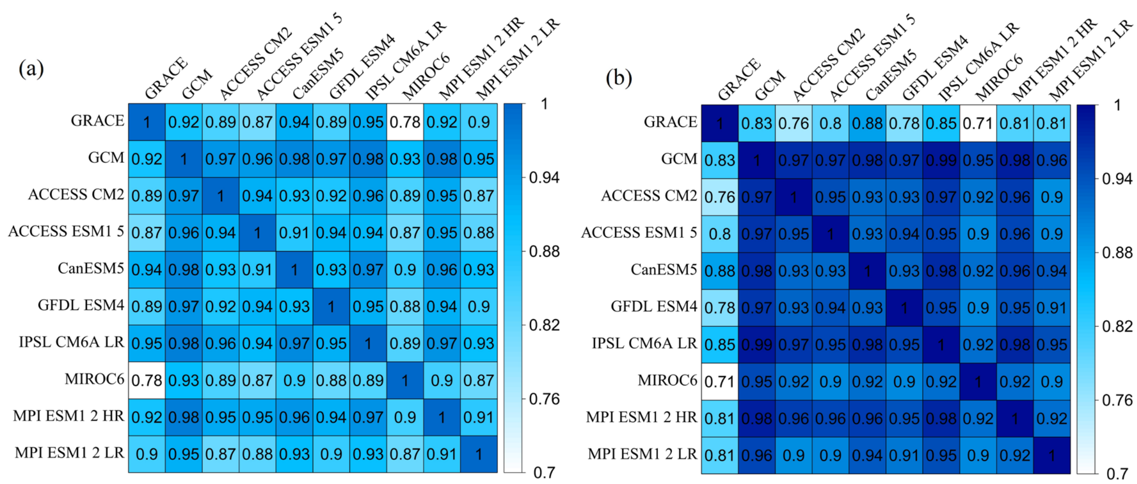


**Figure S7.** Correlation matrix between different GCMs-modelled TWSA and GRACE observations over global land excluding Antarctica and Greenland during April 2002-December 2014 (a) after and (b) before bias correction. Note: The numbers mean the Pearson correlation coefficients between two variables.

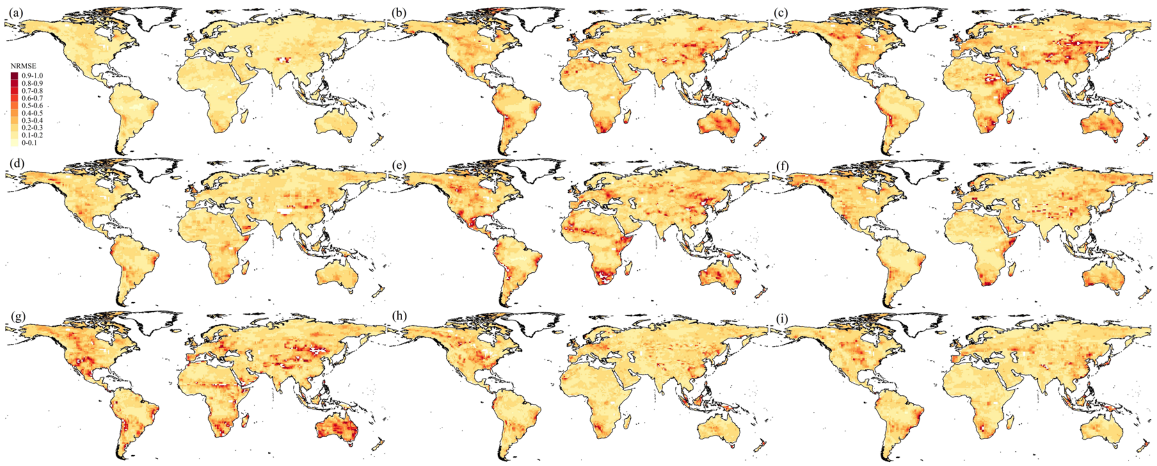


**Figure S8.** Global distribution of NRMSE between TWSA derived from the GRACE mission and each member and the ensemble mean of the eight GCMs before bias correction during the period April 2002-December 2014. The panels (a-i) denotes the results of the ensemble mean, ACCESS-CM2, ACCESS-ESM-1-5, CanESM5, GFDL-ESM4, IPSL-CM6A-LR, MIROC6, MPI-ESM1-2-HR, and MPI-ESM1-2-LR model.

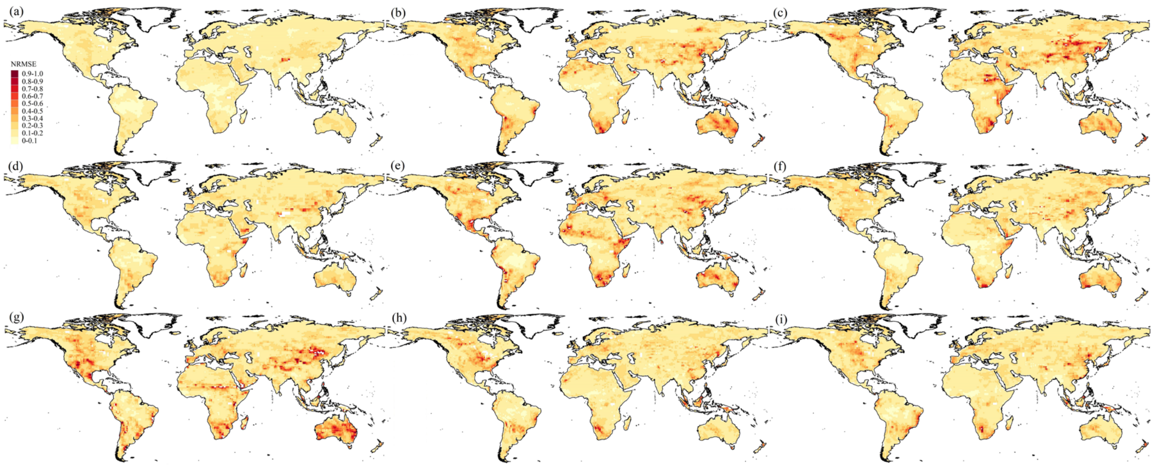

**Figure S9.** Global distribution of NRMSE between TWSA derived from the GRACE mission and each member and the ensemble mean of the eight GCMs after bias correction during the period April 2002-December 2014. The panels (a-i) denotes the results of the ensemble mean, ACCESS-CM2, ACCESS-ESM-1-5, CanESM5, GFDL-ESM4, IPSL-CM6A-LR, MIROC6, MPI-ESM1-2-HR, and MPI-ESM1-2-LR model.

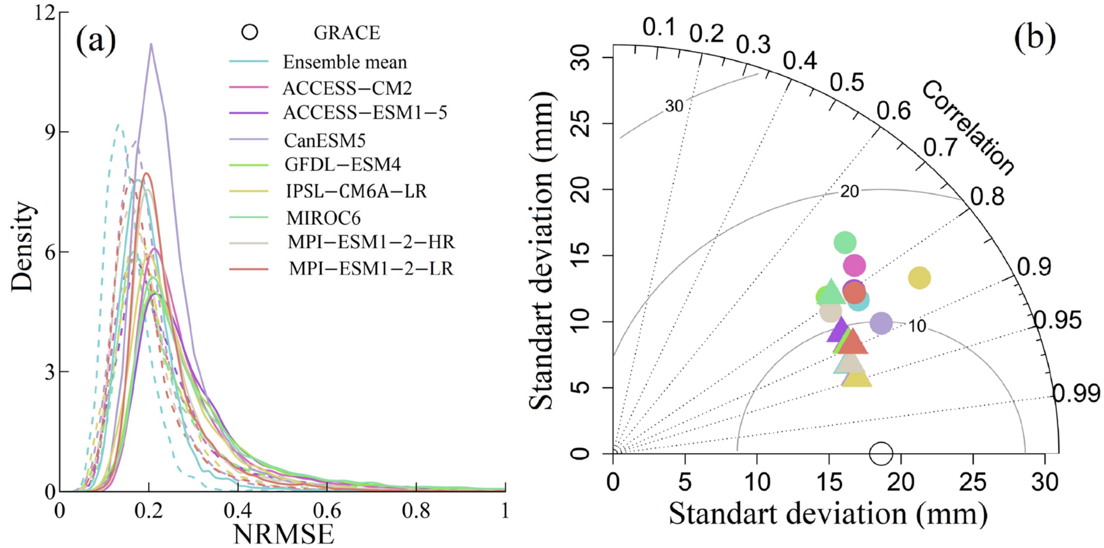


**Figure S10.** (a) Probability density function and (b) Taylor diagram of NRMSE between TWSA derived from the GRACE mission and each member and the ensemble mean of eight GCMs during the period April 2002-December 2014. Solid and dashed lines in sub-figure (a) and corresponding filled circles and triangles in sub-figure (b) denote the original and bias corrected time series.

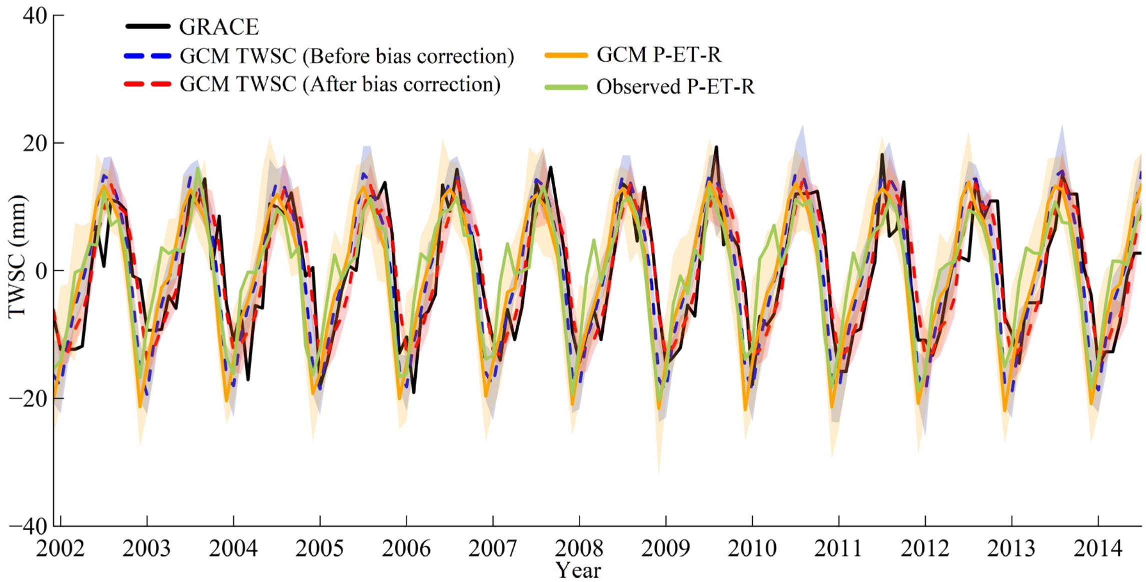


**Figure S11.** Time series of the monthly changes in TWSA (TWSC) and water balance estimates (i.e., P-E-R) derived from GRACE, GCM, and observational products (i.e., P, E, and R) during 2002-2014. Note: The shaded regions represent the spread of the CMIP6 ensemble.

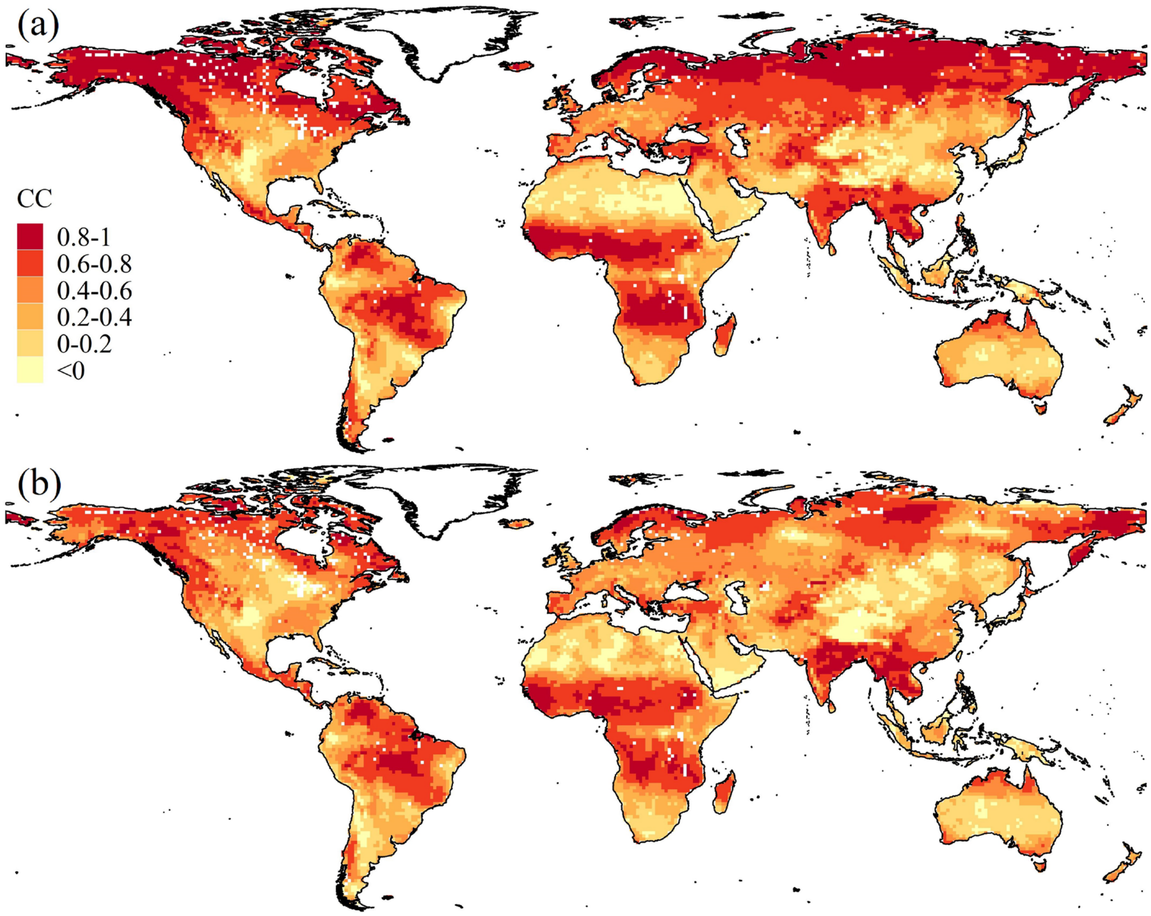


**Figure S12.** Spatial distribution of correlation coefficient between monthly water balance estimates of TWSA changes and the ensemble mean of GCM data (a) before and (b) after bias corrections during 1985-2014. The blank grids indicate the missing values of the datasets.

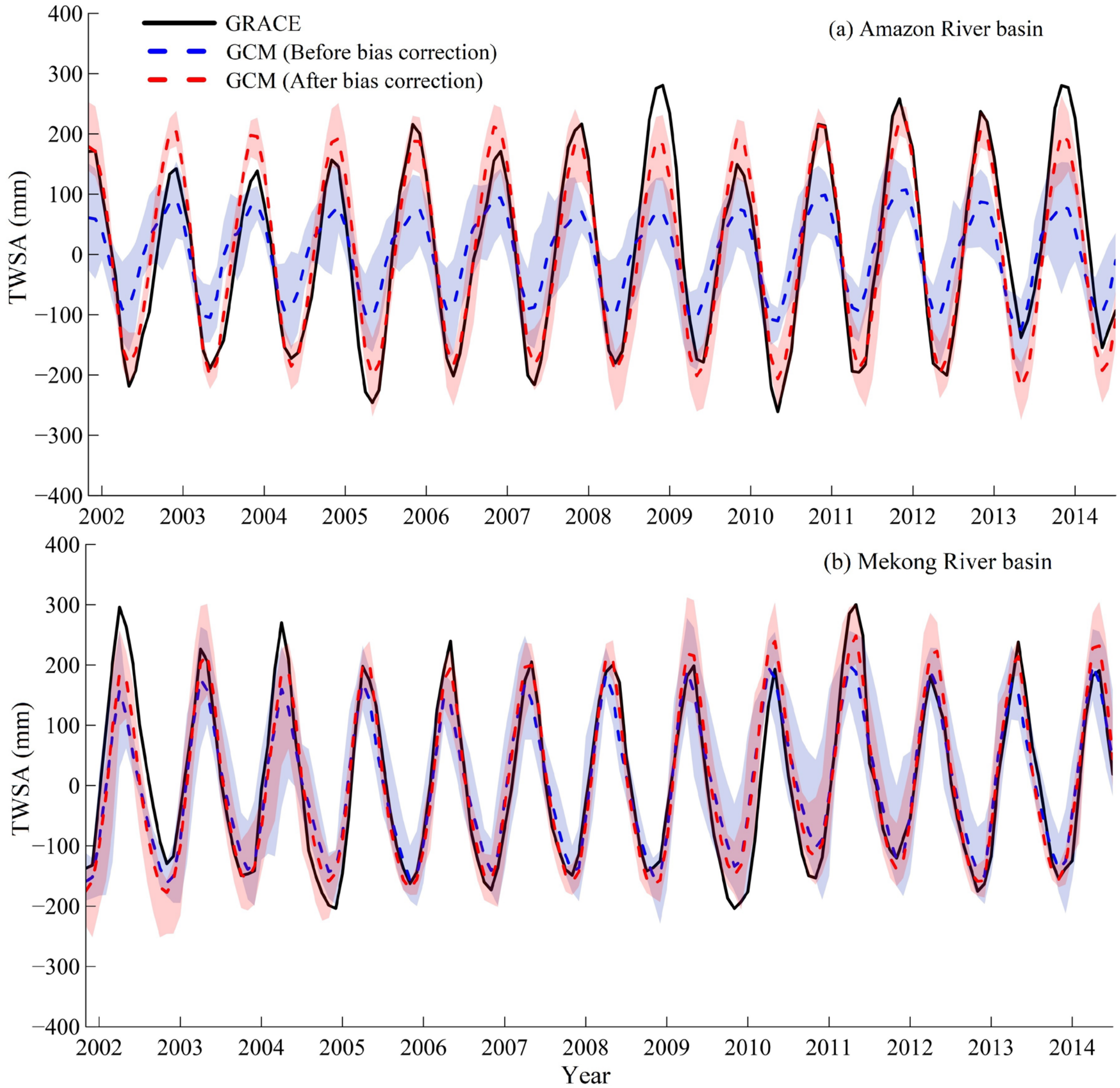


**Figure S13.** Monthly TWSA from GRACE and GCMs with and without bias correction in (a) Amazon and (b) Mekong River basins during 2002-2014. Note: The shading region means the spread of the GCM ensemble.

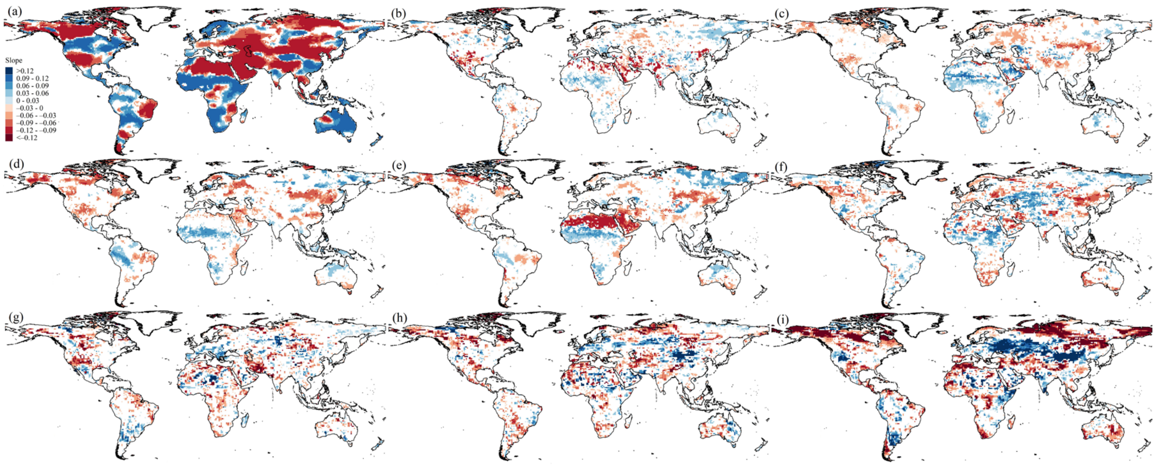


**Figure S14.** Global distribution of the significant ($p<0.05$) long-term trends in TWS-DSI during (a-f) the historical (1985-2014) and future (2071-2100) period under (g) SSP126, (h) SSP245, and (i) SSP585 scenarios. Note: The historical results are based on the (a) GRACE reconstruction, (b) WGHM, (c) VIC, (d) CLSM, (e) Noah, and (f) ensemble mean of eight GCMs, respectively. The future results are based on the ensemble of eight GCMs.

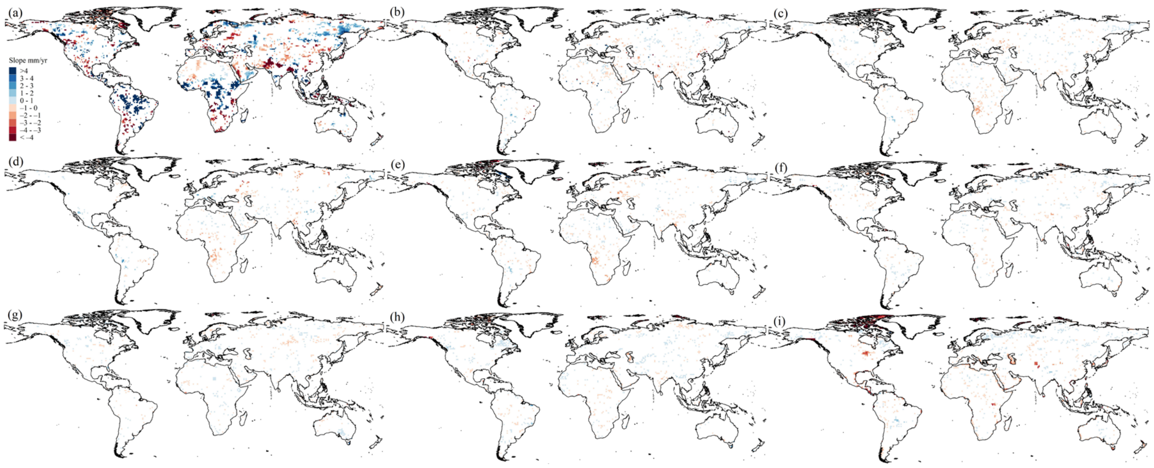


**Figure S15.** Global distribution of the significant ($p<0.05$) long-term trends in P-E-R during (a-f) the historical (1985-2014) and future (2071-2100) period under (g) SSP126, (h) SSP245, and (i) SSP585 scenarios. Note: The historical results are based on the (a) observational products (i.e., CRU P, GLEAM E, and G-RUN R), (b) WGHM, (c) VIC, (d) CLSM, (e) Noah, and (f) ensemble mean of eight GCMs, respectively. The future results are based on the ensemble of eight GCMs.

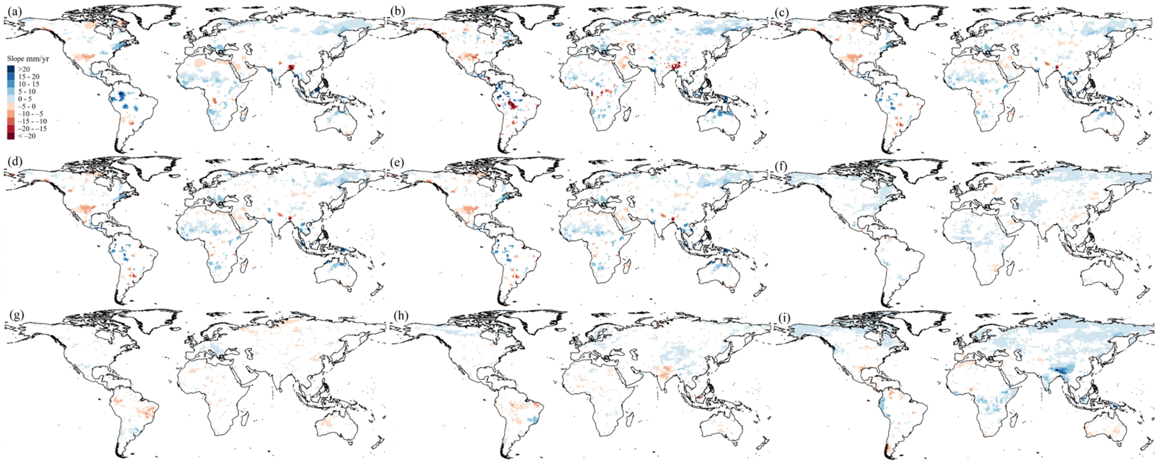


**Figure S16.** Global distribution of the significant ($p<0.05$) long-term trends in P during (a-f) the historical (1985-2014) and future (2071-2100) period under (g) SSP126, (h) SSP245, and (i) SSP585 scenarios. Note: The historical results are based on the (a) CRU, (b) WGHM, (c) VIC, (d) CLSM, (e) Noah, and (f) ensemble mean of eight GCMs, respectively. The future results are based on the ensemble of eight GCMs. The VIC, CLSM, and Noah models are forced by the same precipitation dataset because they are from the GLDAS 2.0 family.

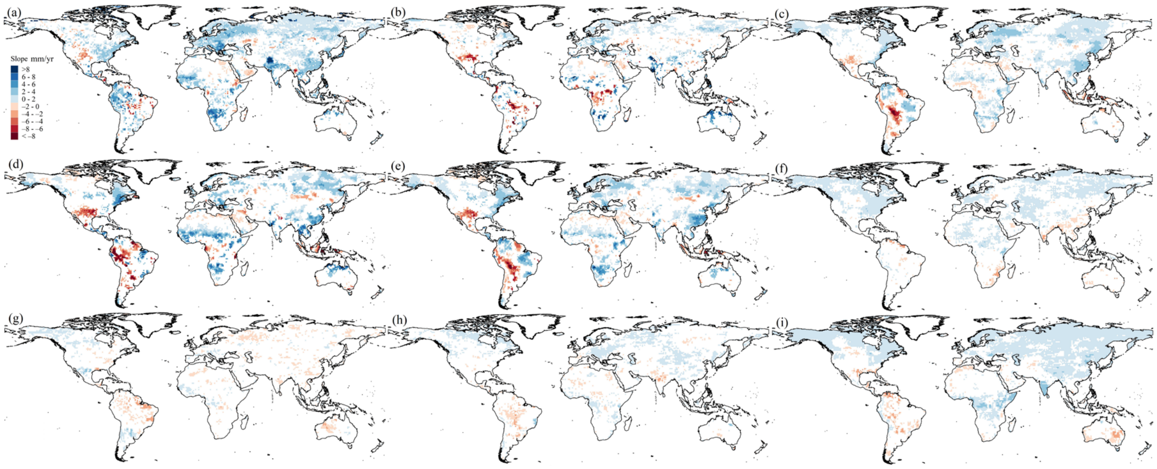


**Figure S17.** Global distribution of the significant ($p<0.05$) long-term trends in E during (a-f) the historical (1985-2014) and future (2071-2100) period under (g) SSP126, (h) SSP245, and (i) SSP585 scenarios. Note: The historical results are based on the (a) GLEAM E, (b) WGHM, (c) VIC, (d) CLSM, (e) Noah, and (f) ensemble mean of eight GCMs, respectively. The future results are based on the ensemble of eight GCMs.

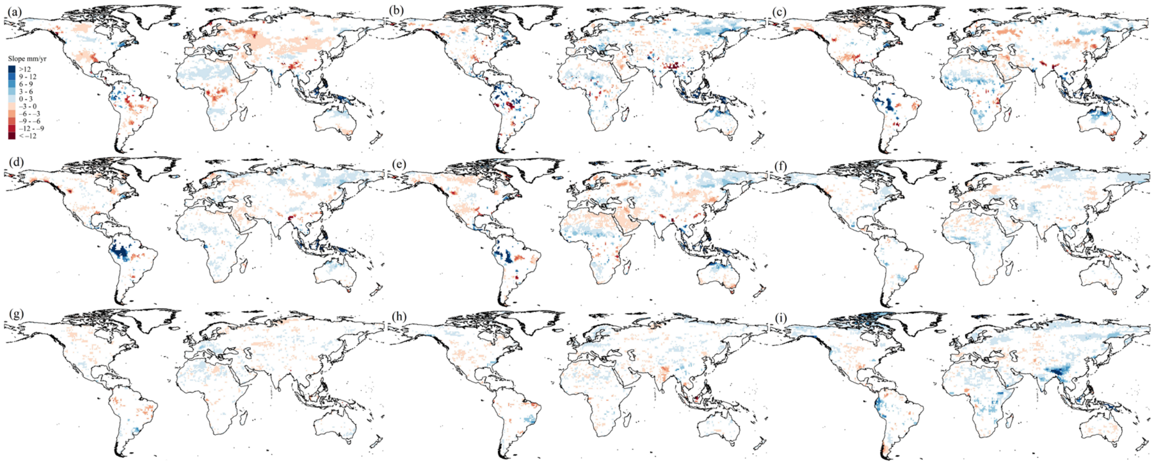


**Figure S18.** Global distribution of the significant ($p<0.05$) long-term trends in R during (a-f) the historical (1985-2014) and future (2071-2100) period under (g) SSP126, (h) SSP245, and (i) SSP585 scenarios. Note: The historical results are based on the (a) G-RUN, (b) WGHM, (c) VIC, (d) CLSM, (e) Noah, and (f) ensemble mean of eight GCMs, respectively. The future results are based on the ensemble of eight GCMs.

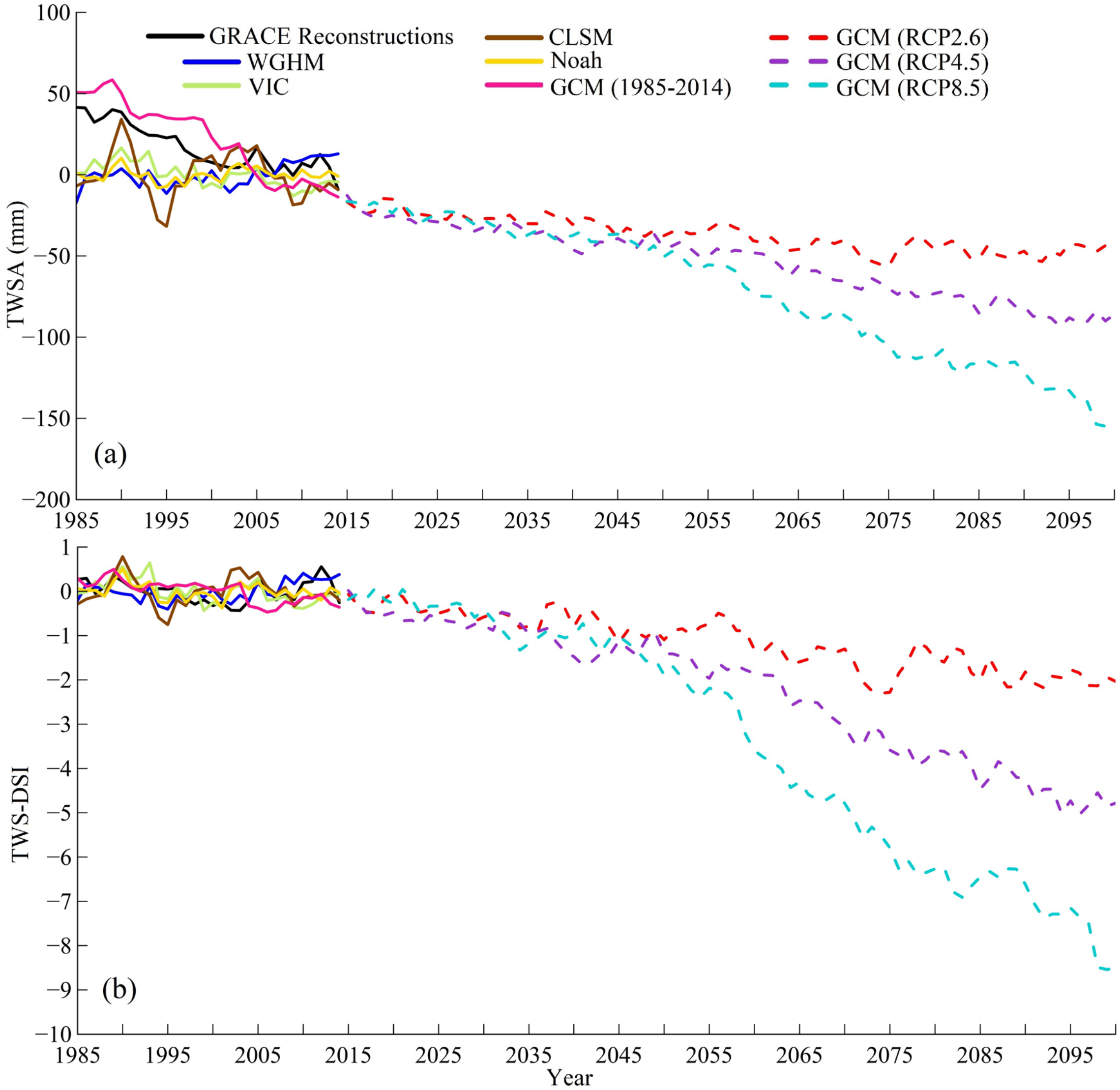


**Figure S19.** Yearly time series of (a) TWSA and (b) TWS-DSI in the QTP during 1985-2100 from different models.

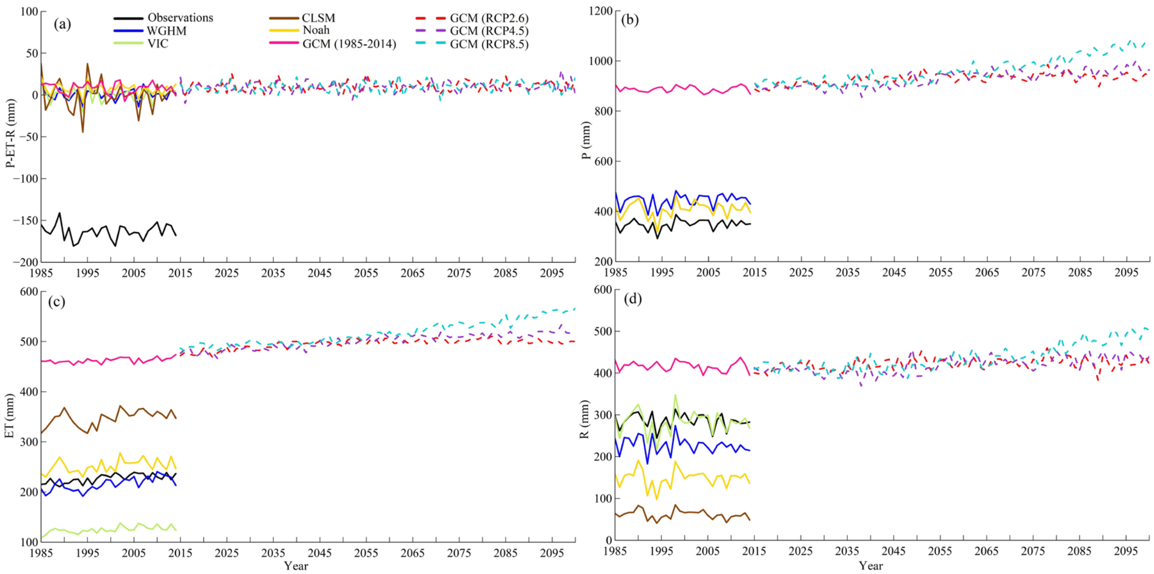


**Figure S20.** Same as Figure S19, but for the (a) P-E-R, (b) P, (c) E, and (d) R. Note: The VIC, CLSM, and Noah models are forced by the same precipitation dataset because they are from the GLDAS 2.0 family.

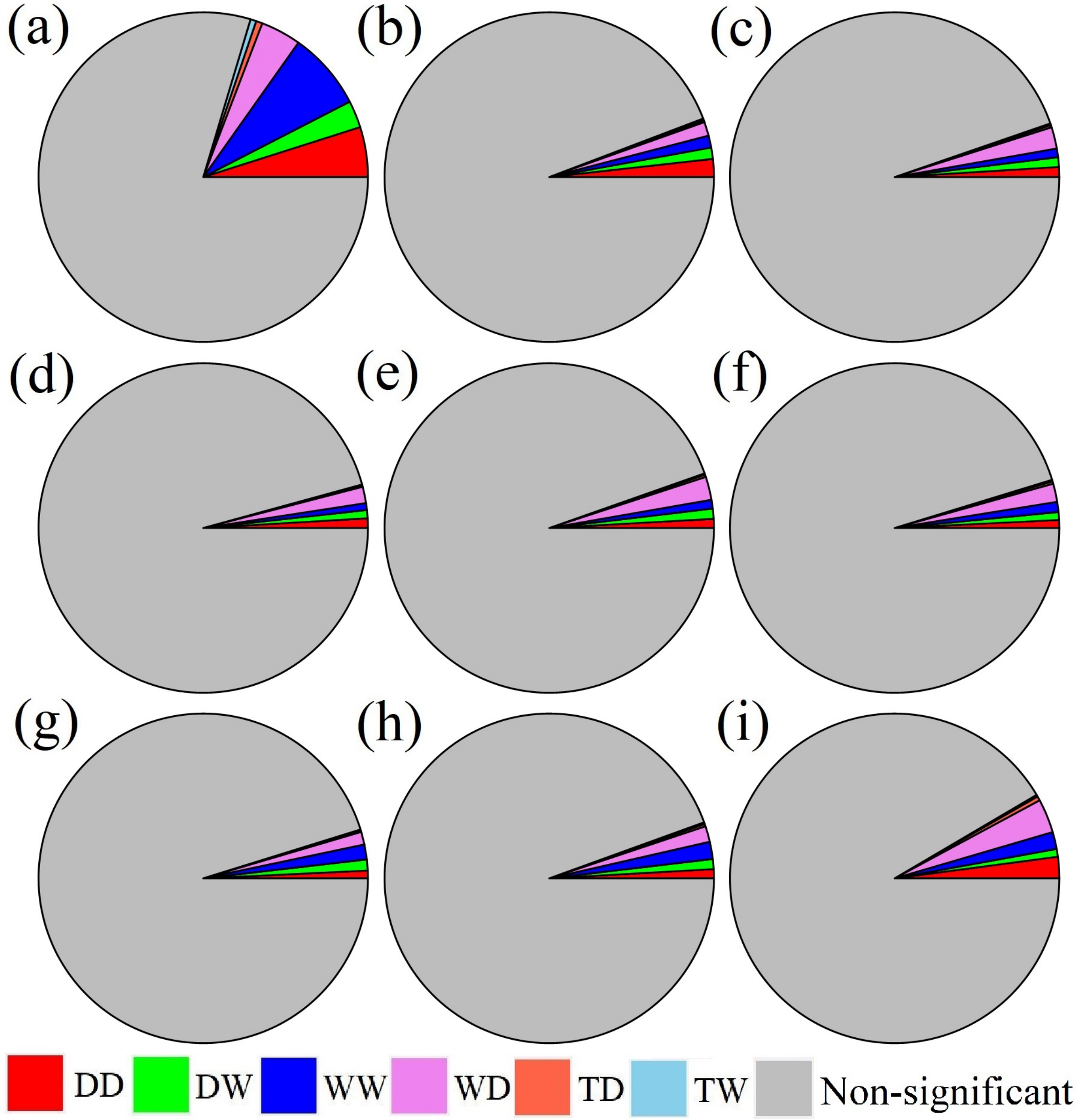

**Figure S21.** Same as the Figure 5, but the metric P-E-R.

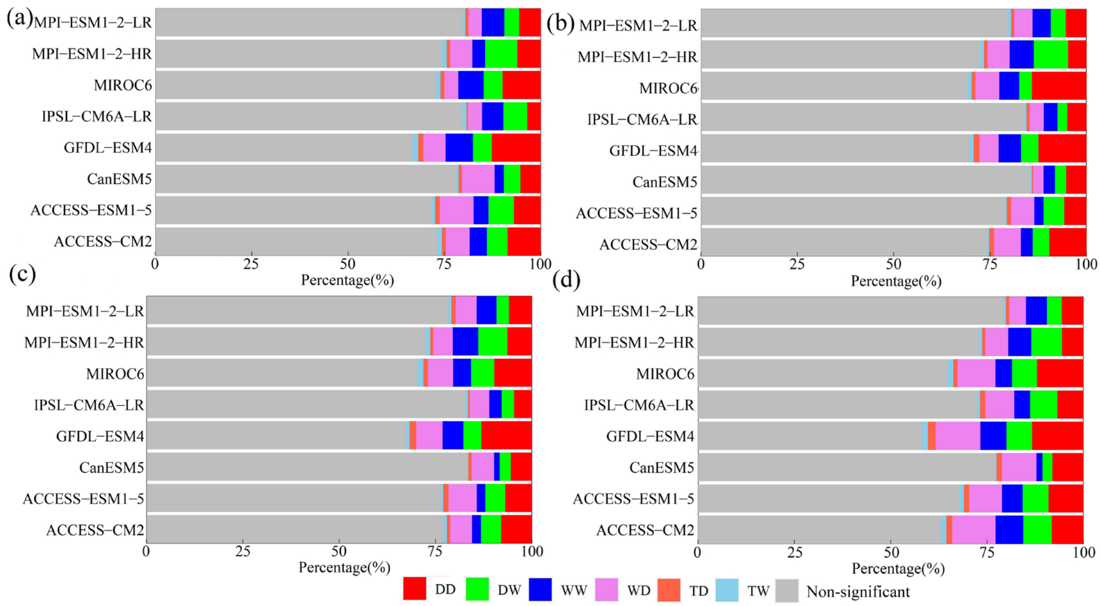


**Figure S22.** Fraction of the global land area showing different patterns using TWS-DSI based on individual GCM models during the (a) historical (1985-2014) and future (2071-2100) period under (b) SSP126, (c) SSP245, and (d) SSP585 scenarios, respectively.

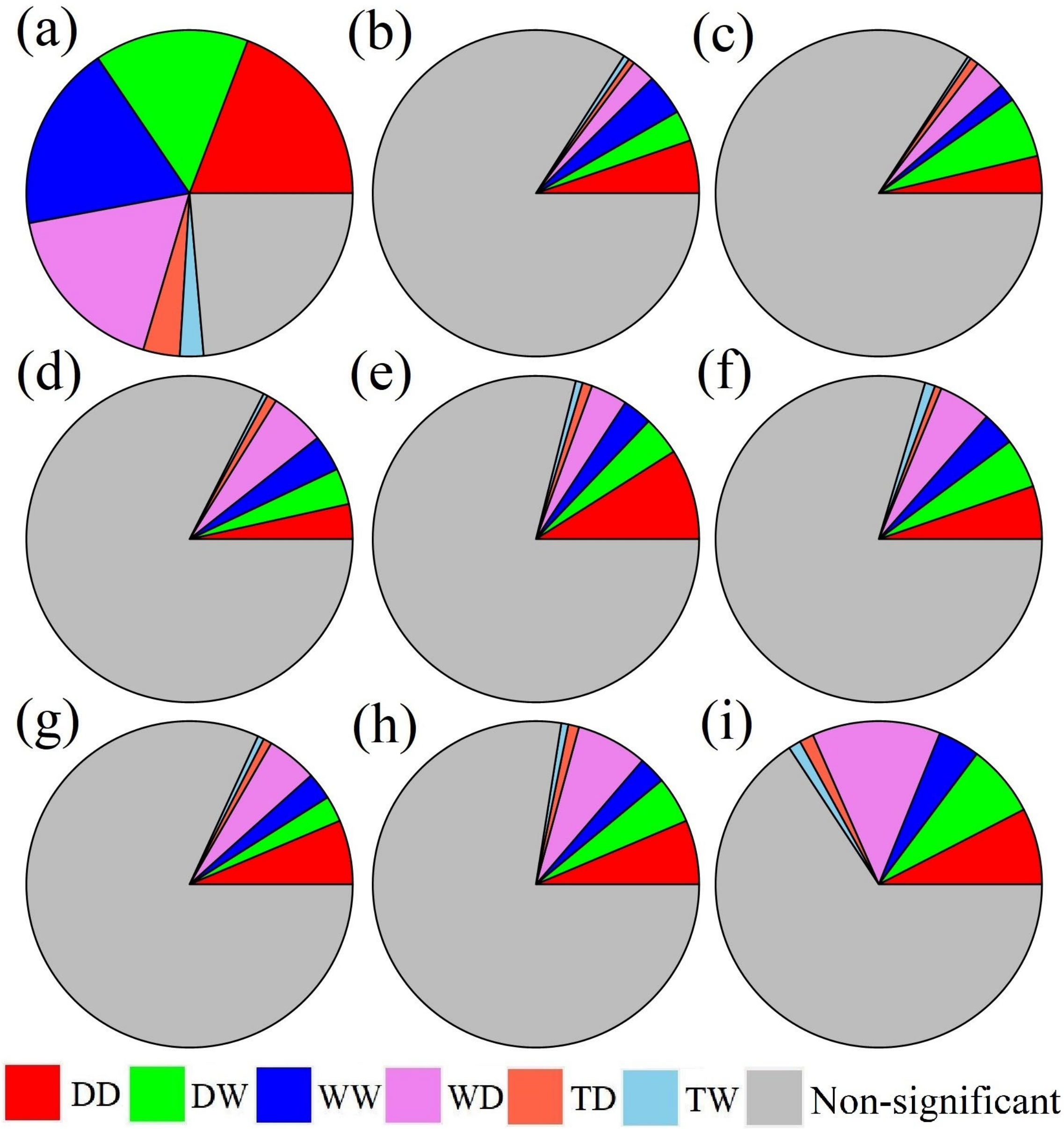


**Figure S23.** Same as the Figure 5, but with a significance of 0.01.

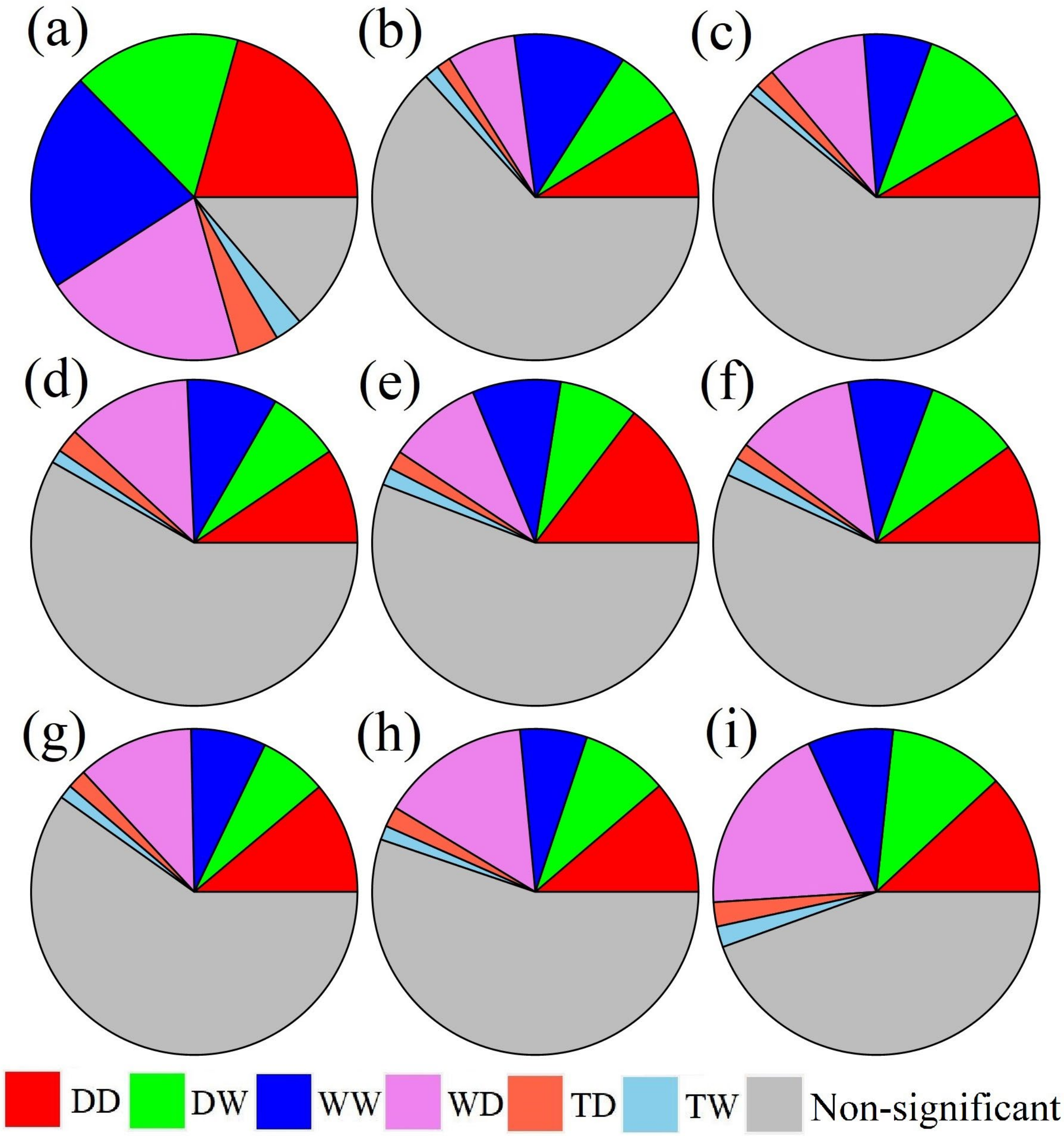

**Figure S24.** Same as the Figure 5, but with a significance of 0.1.

**Table S1.** Summary of attributes of different datasets used in this study.

| Dataset | GRACE | WGHM | VIC | Noah | CLSM | CMIP6 |
|---|---|---|---|---|---|---|
| Parameter | Satellite | GHM | | LSM | | GCM |
| Surface water storage | √ | √ | × | × | × | × |
| Soil moisture | √ | √ | √ | √ | √ | √ |
| Groundwater storage | √ | √ | × | × | √ | × |
| Canopy water | √ | √ | √ | √ | √ | × |
| Snow water | √ | √ | √ | √ | √ | √ |
| Soil layers (no.) | / | 1 | 3 | 4 | 10 | 3~18 |
| Soil depth (m) | / | 2 | 2 | 2 | 1 | 2~10 |

**Table S2.** Standard classification of the TWS-DSI (Zhao et al., 2017).

| Category | Description | TWS-DSI |
| --- | --- | --- |
| W4 | Exceptionally wet | 2 or greater |
| W3 | Extremely wet | 1.6 to 1.99 |
| W2 | Very wet | 1.3 to 1.59 |
| W1 | Moderately wet | 0.8 to 1.29 |
| W0 | Slightly wet | 0.5 to 0.79 |
| WD | Near normal | 0.49 to -0.49 |
| D0 | Abnormally dry | -0.5 to -0.79 |
| D1 | Moderate dry | -0.8 to -1.29 |
| D2 | Severe dry | -1.3 to -1.59 |
| D3 | Extreme dry | -1.6 to -1.99 |
| D4 | Exceptional dry | -2 to less |

**Table S3.** Percentage of the global land area with different patterns during the historical (1985-2014) and future (2071-2100) periods. Note: DD indicates the dry gets drier; DW indicates the dry gets wetter; WW indicates the wet gets wetter; WD indicates the wet gets drier; TD indicates the transition gets drier; TW indicates the transition gets wetter; Non-significant indicates the regions showing non-significant ($p>0.05$) trends in TWS-DSI.

| Model/data set | GRACE Reconstruction | WGHM | VIC | CLSM | Noah | GCM (historical period) | GCM (SSP126) | GCM (SSP245) | GCM (SSP585) |
|---|---|---|---|---|---|---|---|---|---|
| DD | 20.17% | 7.32% | 6.47% | 7.33% | 12.42% | 8.18% | 9.28% | 9.37% | 10.32% |
| DW | 16.13% | 5.42% | 9.21% | 5.82% | 6.29% | 7.59% | 5.03% | 7.03% | 9.90% |
| WW | 20.67% | 8.00% | 4.54% | 6.94% | 6.53% | 6.23% | 5.38% | 4.89% | 6.76% |
| WD | 19.30% | 4.79% | 7.19% | 9.45% | 6.96% | 9.17% | 8.81% | 11.69% | 16.74% |
| TD | 3.88% | 0.95% | 1.49% | 1.63% | 1.49% | 1.15% | 1.43% | 1.66% | 1.98% |
| TW | 2.63% | 1.10% | 0.73% | 0.94% | 1.27% | 1.56% | 1.07% | 1.09% | 1.76% |
| Non-significant | 17.20% | 72.42% | 70.36% | 67.89% | 65.04% | 66.11% | 69.01% | 64.28% | 52.55% |

**Table S4.** Same as Table S3, but for the metric P-E-R.

| Model/data set | Observation -based product | WGHM | VIC | CLSM | Noah | GCM (historical period) | GCM (SSP126) | GCM (SSP245) | GCM (SSP585 ) |
|---|---|---|---|---|---|---|---|---|---|
| DD | 4.91% | 1.76% | 0.98% | 0.94% | 0.89% | 0.78% | 0.75% | 0.89% | 2.10% |
| DW | 2.65% | 1.11% | 0.95% | 0.80% | 1.00% | 0.78% | 1.08% | 0.98% | 0.76% |
| WW | 7.63% | 1.18% | 0.85% | 0.67% | 0.86% | 0.99% | 1.46% | 1.69% | 1.67% |
| WD | 3.97% | 1.37% | 2.11% | 1.61% | 2.28% | 1.80% | 1.26% | 1.55% | 3.33% |
| TD | 0.63% | 0.19% | 0.22% | 0.16% | 0.23% | 0.23% | 0.09% | 0.23% | 0.41% |
| TW | 0.57% | 0.17% | 0.17% | 0.07% | 0.13% | 0.15% | 0.15% | 0.17% | 0.19% |
| Non-significant | 79.63% | 94.22% | 94.72% | 95.74% | 94.62% | 95.27% | 95.21% | 94.48% | 91.54% |

**Table S5.** Same as Table S3, but for the difference between the DDWW test results under the 0.01 and 0.05 significance levels.

| Model/dataset | GRACE Reconstructions | WGHM | VIC | CLSM | Noah | GCM (historical period) | GCM (SSP126) | GCM (SSP245) | GCM (SSP585) |
|---|---|---|---|---|---|---|---|---|---|
| DD | -0.98% | -2.06% | -2.78% | -3.86% | -3.40% | -2.92% | -2.91% | -3.00% | -2.73% |
| DW | -0.84% | -2.36% | -3.19% | -2.24% | -2.45% | -2.68% | -2.46% | -2.40% | -2.74% |
| WW | -2.23% | -3.93% | -2.79% | -3.34% | -3.62% | -2.92% | -2.70% | -2.19% | -2.63% |
| WD | -1.81% | -2.43% | -4.04% | -3.99% | -3.31% | -3.94% | -3.79% | -4.64% | -4.00% |
| TD | -0.27% | -0.36% | -0.64% | -0.67% | -0.52% | -0.49% | -0.58% | -0.59% | -0.57% |
| TW | -0.30% | -0.52% | -0.41% | -0.52% | -0.58% | -0.54% | -0.45% | -0.39% | -0.54% |
| Non-significant | 6.42% | 11.65% | 13.84% | 14.61% | 13.89% | 13.48% | 12.88% | 13.21% | 13.20% |

**Table S6.** Same as Table S3, but for the difference between the DDWW test results under the 0.1 and 0.05 significance levels.

| Model/dataset | GRACE Reconstruction | WGHM | VIC | CLSM | Noah | GCM (historical period) | GCM (SSP126) | GCM (SSP245) | GCM (SSP585) |
|---|---|---|---|---|---|---|---|---|---|
| DD | 0.52% | 1.46% | 1.97% | 2.14% | 2.23% | 1.82% | 1.85% | 1.89% | 1.60% |
| DW | 0.48% | 1.75% | 1.85% | 1.42% | 1.54% | 1.79% | 1.71% | 1.59% | 1.54% |
| WW | 1.13% | 3.12% | 2.19% | 2.04% | 2.24% | 2.16% | 2.07% | 1.74% | 1.72% |
| WD | 0.98% | 1.98% | 2.64% | 2.94% | 2.39% | 2.80% | 2.76% | 3.17% | 2.45% |
| TD | 0.20% | 0.45% | 0.44% | 0.73% | 0.35% | 0.43% | 0.46% | 0.36% | 0.43% |
| TW | 0.09% | 0.38% | 0.37% | 0.39% | 0.46% | 0.30% | 0.31% | 0.31% | 0.31% |
| Non-significant | -3.39% | -9.14% | -9.47% | -9.66% | -9.22% | -9.28% | -9.16% | -9.06% | -8.04% |

Reference:

Beck, H. E., Zimmermann, N. E., McVicar, T. R., Vergopolan, N., Berg, A., and Wood, E. F.: Present and future Köppen-Geiger climate classification maps at 1-km resolution, Sci. Data, 5, https://doi.org/10.1038/sdata.2018.214, 2018.

Zhao, M., Geruo, A., Velicogna, I., and Kimball, J. S.: Satellite Observations of Regional Drought Severity in the Continental United States Using GRACE-Based Terrestrial Water Storage Changes, J. Clim., 30, 6297–6308, https://doi.org/10.1175/JCLI-D-16-0458.1, 2017.